Swiss Journal of Geosciences (2018) 111:341–352
https://doi.org/10.1007/s00015-017-0296-x

Integrated foraminifera and $\delta^{13}C$ stratigraphy across the Cenomanian–Turonian event interval in the eastern Baltic (Lithuania)

Agnė Venckutė-Aleksienė[1] · Andrej Spiridonov[2] · Andrius Garbaras[3] · Sigitas Radzevičius[2]

Received: 6 October 2017 / Accepted: 21 December 2017 / Published online: 9 February 2018

Abstract
The Cenomanian–Turonian transition marks one of the most important extinction episodes of the Mesozoic era. This extinction event was associated with the development of widespread oceanic anoxia and pronounced stable carbon isotopic excursion. Despite its importance, the effects of the perturbation on higher latitude biotas, and from the Baltic region in particular, are currently underexplored. Therefore, in this contribution we present the fossil record of a foraminifera succession integrated with $\delta^{13}C$ trends from two deep cores: Bliūdsukiai-19 from western Lithuania and Baltašiškė-267 from southern Lithuania. Two foraminiferal zones were distinguished: *Rotalipora cushmani* from the upper Cenomanian and *Whiteinella archaeocretacea* from the boundary strata between the Cenomanian and Turonian in the Baltašiškė-267 core section, and a *W. archaeocretacea* Zone in the Bliūdsukiai-19 core section. A chemostratigraphical analysis of the stable carbon isotopes revealed a positive Cenomanian–Turonian $\delta^{13}C$ anomaly, with maximum values reaching 3.57‰ in the upper part of the Bliūdsukiai-19 core section. A non-metric multidimensional scaling analysis of the foraminifera communities revealed that the major changes in their assemblages were strongly temporally organized and associated with the changes in the stable carbon isotopic ratios. This fact points to the significant effects of the C–T extinction event on the northern Neotethys paleocommunities.

Keywords Foraminifera · Cretaceous · Cenomanian-Turonian boundary · $\delta^{13}C$ stratigraphy

1 Introduction

The transition between the Cenomanian and Turonian epochs was marked by one of the most significant species extinctions and radiations, as well as the anoxic and stable carbon isotopic events of the Upper Cretaceous period (Fraass et al. 2015; Harries and Little 1999; Hart 1999; Hart and Leary 1991; Jarvis et al. 2011; Kauffman and Hart 1996; Keller and Pardo 2004; Schlanger and Jenkyns 1976). It is estimated from the global taxonomic data-set that the Cenomanian–Turonian extinction event (C–T event) eliminated up to eight percent of marine animal families (Kauffman and Hart 1996; Sepkoski 1993). According to material from the best-studied sections in the world, from the Western Interior Basin, the discussed event proceeded as a complex hierarchical superposition of smaller scale events of differing temporal and spatial significance (Sageman et al. 1997). Estimates show that losses of marine mollusc species during two impulses of the event sequentially eliminated one half and one-third of the species for each decimation episode (Kauffman and Hart 1996). Some analyses of regional (Western Interior) biotas show that macroinvertebrates sustained up to 79% species extinction (Harries and Little 1999), with nektobenthic ammonites affected more severely than other groups (Elder 1989). In the Caucasus region, the discussed C–T event had a severe and long-term biodiversity dampening effect, decreasing the

Editorial handling: D. Marty.

Electronic supplementary material The online version of this article (https://doi.org/10.1007/s00015-017-0296-x) contains supplementary material, which is available to authorized users.

✉ Andrej Spiridonov
andrej.spiridonov@gf.vu.lt

[1] Laboratory of Bedrock Geology, Nature Research Centre, Akademijos Str. 2, 08412 Vilnius, Lithuania

[2] Department of Geology and Mineralogy, Faculty of Chemistry and Geosciences, Vilnius University, 03101 Vilnius, Lithuania

[3] Department of Nuclear Research, Center for Physical Sciences and Technology, 10221 Vilnius, Lithuania

standing invertebrate diversity for the entire succeeding Turonian (Ruban et al. 2011). In the American sections there was a distinct episode of terminations of old taxa and later proliferations of new taxa of low oxygen tolerant inoceramid bivalves (Harries 2003). A very similar pattern of decimation and diversity rebound of this group was found in data from Japan (Takahashi 2005). Approximately one-third of the old foraminifera species in a type locality of the Cenomanian–Turonian transition in the Pueblo section (Colorado) were replaced by an essentially equal number of new species (Keller and Pardo 2004). On the other hand, there was a much smaller species turnover in the foraminifera in higher latitudes, which points to the geographical selectivity of the mass extinction (Keller et al. 2001). The Cenomanian–Turonian transition also marked one of the most important extinctions (Bardet 1994), as well as evolutionary radiation (Bardet et al. 2008) events of marine reptiles during the Mesozoic. It was suggested that the elevated extinction rates in marine reptiles during the C–T transition could have been, at least partially, influenced by sampling artefacts (Benson et al. 2010), although later on the entire approach used by the cited authors was contested for its validity (Sakamoto et al. 2017); therefore, the extinction pattern in marine tetrapods is most probably real. The terrestrial realm was also apparently affected by the transition, as in the North American record there was a simultaneous reduction in the order, family, and genus-level diversities of nonmarine vertebrates (Eaton and Kirkland 2003), with aquatic nonmarine forms possibly suffering a greater impact (Eaton et al. 1997). The biostratigraphically constrained positive stable carbon isotopic anomaly, which developed in the vicinity of the C–T transition, is globally detectable in both organic carbon deposits and carbonates, which shows the global biogeochemical character of the oceanic perturbation (Gale et al. 1993; Hasegawa and Saito 1993; Schlanger et al. 1987; Tsikos et al. 2004). The onset and duration of the C–T event (and the boundary between the stages), thanks to the numerical integration of radiogeochronological, astrochronological, and chemo- and biostratigraphical data and models, can be estimated with great precision (Sageman et al. 2006). The latest estimates put the date for the C/T boundary from 93.90 ± 0.15 Ma (Meyers et al. 2012) up to 94.10 ± 0.15 Ma (Batenburg et al. 2016), with a probable duration of the positive carbon isotopic excursion and OAE 2 (Ocean Anoxic Event II) of 847–885 Ka (Sageman et al. 2006).

There are several propositions for the ultimate causes of the C–T mass extinction event. The explanations range from the effects of repeated asteroid or comet impacts (Kauffman and Hart 1996; Orth et al. 1993) to perturbations in biogeochemical cycles caused by changes in oceanic spreading rates and/or the development of large igneous provinces. The latter explanation is the most plausible because of the abundant evidence (Jenkyns et al. 2017; Kerr 1998; Orth et al. 1993; Sinton and Duncan 1997). In addition, there is growing support for the proposition that the fine structure of the event with its multiple turnovers (Batenburg et al. 2016), or at least its ending, (Li et al. 2017) was modulated by the Earth's orbital (Milankovitch) cycles (Prokoph et al. 2001; Sageman et al. 1998).

Although there is a large body of work dedicated to understanding the OAE 2 and its geobiological consequences, the northern part of the Tethys (i.e., the Baltic region) is currently underexplored in terms of stratigraphy and paleoecology. Therefore, in this contribution we present an integrated foraminiferal biostratigraphical and stable carbon isotopic analysis of two shallow water successions from Lithuanian territory, the Bliūdsukiai-19 and Baltašiškė-267 deep core sections. The stratigraphical data were supported by a quantitative analysis of foraminiferal species occurrences. In addition, we revealed changes in the prevalence of the coiling directions in the long-ranging planktonic foraminiferal species *Muricohedbergella delrioensis*, which was previously proposed as a valuable paleoceanographical proxy (Desmares et al. 2016).

2 Geological setting

The described material comes from the Bliūdsukiai-19 well, which is located in the south-western facies zone and from the Baltašiškė-267 well, which is located in the southern facial zone of the C–T deposits. (Figure 1a, b). The southern facial zone represents relatively deeper environments than the south-western facial zone. Accordingly, it is expected that the Cretaceous geological section is more complete in southern Lithuania.

The studied area corresponds paleogeographically to the northern shallow water part of the Neotethys ocean (Ogg et al. 2012). Upper Cretaceous sedimentary rocks in the Lithuania form continuous and complete (at the stage level) stratigraphic succession, with comfortable transition in to the Paleogene strata (Paškevičius 1997). The chronostratigraphic subdivision of the upper Cretaceous in Lithuania and the surrounding territories are mostly based on foraminifera biostratigraphy (Grigelis and Leszczyński 1998), but also on the distributions of other faunal groups including selachians and bivalves (Adnet et al. 2008; Dalinkevičius 1935; Paškevičius 1997). The Cenomanian strata are subdivided into three formations. The Labguva formation, which contains almost the entire Cenomanian, is distinguished in the western facies zones of the south-eastern Baltic. In the upper part (studied here) it is composed of fine-grained clastic sediments with abundant glauconite. The Akmuo formation is distinguished in the lower Cenomanian strata of the south and north-eastern

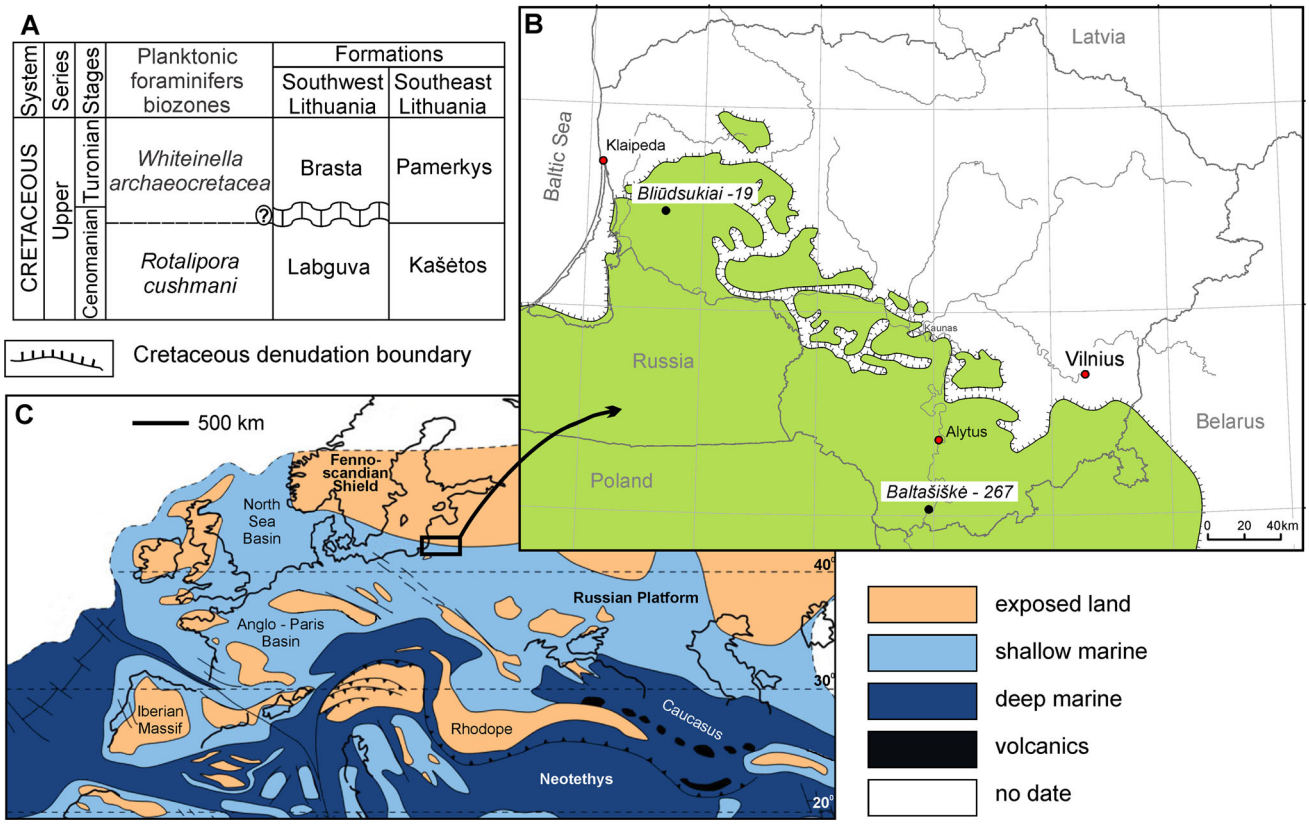

Fig. 1 **a** Stratigraphy of the Cenomanian–Turonian boundary in Lithuania (after Paškevičius 1997); **b** Distribution of Cretaceous deposits in Lithuania (Grigelis and Leszczyński 1998) and borehole locations; **c** Palaeogeography of the northern Tethyan margin during the Cenomanian age (Philip et al. 2000; Sachs et al. 2017)

facies zones, and is composed of carbonatic glauconitic sands and silts. The upper Cenomanian strata from the same eastern facies zones are combined with the Kašėtos formation and are mostly composed of marls and sands of varying compositions with abundant phosphorite concretions (Paškevičius 1997). The lower Turonian strata are subdivided into two formations—the Brasta formation is distinguished in the western facies zones and is composed of marls and siltstones. The Pamerkys formation is distinguished in the eastern facies zones and is composed of chalk and chalky marls (Grigelis 1996).

In this contribution the Kašėtos and the Pamerkys formations were distinguished in the investigated interval of the Baltašiškė-267 well. The Kašėtos formation is composed of glauconitic sand and sandstone in the upper part of the formation. The Pamerkys formation is composed of argillaceous limestone with chalk interbeds in the Baltašiškė-267 well. The Brasta formation is distinguished in the studied interval of the Bliūdsukiai-19 well. This formation is mostly composed of argillaceous silt. According to the chronostratigraphical dating, the Kašėtos formation corresponds to the late Cenomanian age (Fig. 1), both the Pamerkys and the Brasta formations corresponds to the late Cenomanian to early Turonian ages.

3 Materials and methods

Rock samples from the Cenomanian–Turonian boundary were collected from two boreholes: Baltašiškė-267 and Bliūdsukiai-19. The Bliūdsukiai-19 borehole represents the Klaipėda facies zone defined in western Lithuania and the Baltašiškė -267 borehole is located in the Kaunas zone in mid-south-eastern Lithuania (Fig. 1). A total of 23 samples from the two cores were analyzed: 11 from the Baltašiskė-267 core and 12 from the Bliūdsukiai-19 core. The samples were collected and analyzed for a foraminiferal faunal diversity estimation and a *Muricohedbergella delrioensis* left and right-coiled morphotype determination. The samples were taken every 1 m where possible. The foraminiferans were extracted by drying the samples, which weighed 50 g each, and later soaking in sodium bicarbonate and washing through a 0.063 mm sieve using standard methods.

For the statistical analysis of the coiling directions of the *M. delrioensis*, at least 100 specimens of this species were evaluated in each sample. The low trochospiral *M. delrioensis* test with 4.5–5.5 globular chambers on the last whorl were observed on the spiral side. The specimens that were coiled in a clockwise direction represented a right-

coiling morphotype and those that were coiled in an anticlockwise direction represented a left-coiling morphotype. This morphological proxy (proportion of dextral and sinistral morphotypes), as shown in previous studies, can be used as an indicator of changing oceanographic conditions (Desmares et al. 2016).

The microphotographs of the representative planktonic and benthic foraminiferal taxa were taken using a scanning electron microscope at the Nature Research Centre (Vilnius, Lithuania). Overall, 24 planktonic species from 10 genera and 6 benthic foraminiferal species and 13 genera were identified in the middle Cenomanian-lower Turonian sedimentary succession (Fig. 2). The most important foraminifera are illustrated in Figs. 3 and 4. The studied specimens are stored in the Museum of Geology at Vilnius University in Lithuania.

For the purpose of the statistical analysis of the foraminiferal communities, the squared root transformed relative abundances of the identified species or genera were used in a non-metric multidimensional scaling (NMDS) procedure with the Bray–Curtis distance [as recommended in Yasuhara et al. (2012)]. The NMDS procedure iteratively reveals the community gradients, without implicitly assuming the shapes of the species distributions along the environmental gradient (Patzkowsky and Holland 2012), which makes this technique eminently suitable for analyzing heterogenous species assemblages. *Muricohedbergella delrioensis* was eliminated from the overall data set due to its low abundance variance, as the sediments were searched for other species until the needed census level of this species (100 specimens) was reached, except for several samples where this species was extremely rare. The samples from both the studied cores were pooled in a common ecological analysis. Later on, the NMDS1 axis, which reveals the strongest association gradient, was used as an explanatory variable that revealed the compositional evolution of the communities through time. The analysis was performed using the metaMDS 'vegan' package function in the R statistical computing environment (Oksanen et al. 2015; R 2015).

The stable carbon and oxygen isotope ratio values from the carbonate fractions were measured at the Mass Spectrometry Laboratory at the Center for Physical Sciences and Technology (Vilnius, Lithuania) using a Thermo Gasbench II coupled with a Thermo Delta V isotope ratio mass spectrometer. Each sample was loaded into 10 ml Labco Exetainer® vials, flushed with He, and later treated with 99.99% H_3PO_4 at 50 °C for 10 h. The isotope data were normalized against the reference materials IAEA-CO-8 ($\delta^{13}C = -5.764 \pm 0.032‰$, $\delta^{18}O = -22.7 \pm 0.2‰$) and NBS 18 ($\delta^{13}C = -5.014 \pm 0.035‰$, $\delta^{18}O = -23.2 \pm 0.1‰$). The standard deviation (1 sigma) for the sample analyses was 0.06‰ for $\delta^{13}C$ and 0.12‰ for $\delta^{18}O$. The results are reported in δ-notation, and the $\delta^{18}O$ and $\delta^{13}C$ values are given as parts per-mil (‰) to V-PDB. For the stratigraphy, only the $\delta^{13}C$ values were analyzed.

4 Results and discussion

4.1 Biostratigraphy

The studied succession is marked by moderately diverse and usually abundant and well-preserved planktonic and

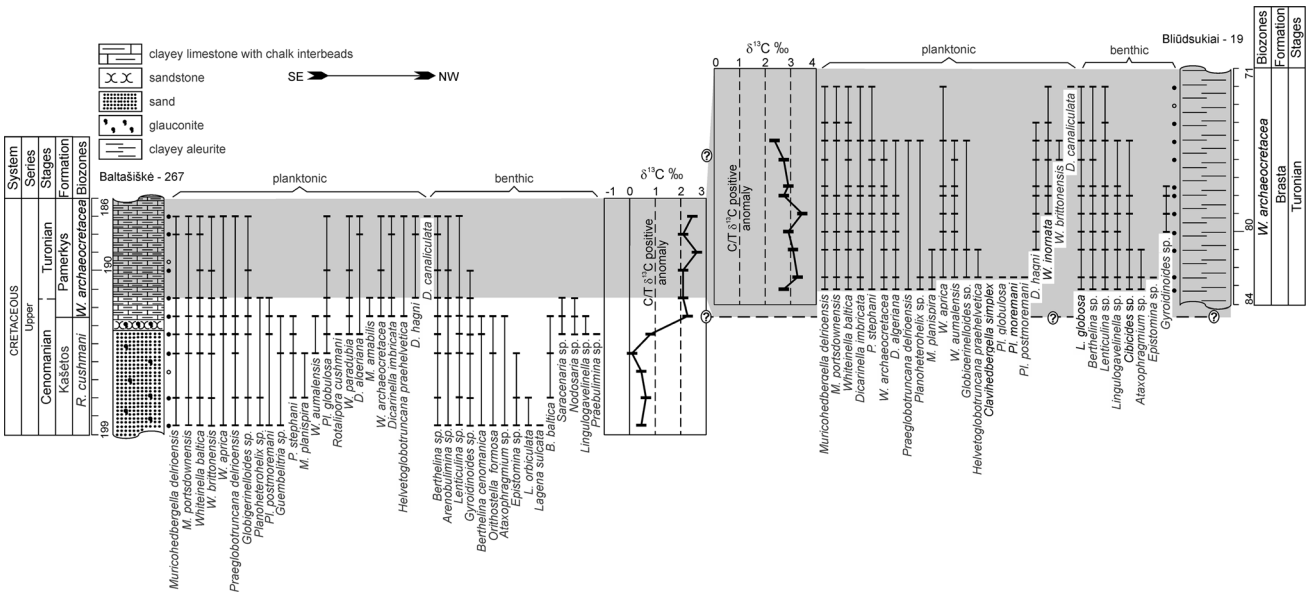

Fig. 2 Stratigraphy, lithology, and distribution of the foraminifera, and the $\delta^{13}C$ trends in the Baltašiškė-267 and the Bliūdsukiai-19 core sections

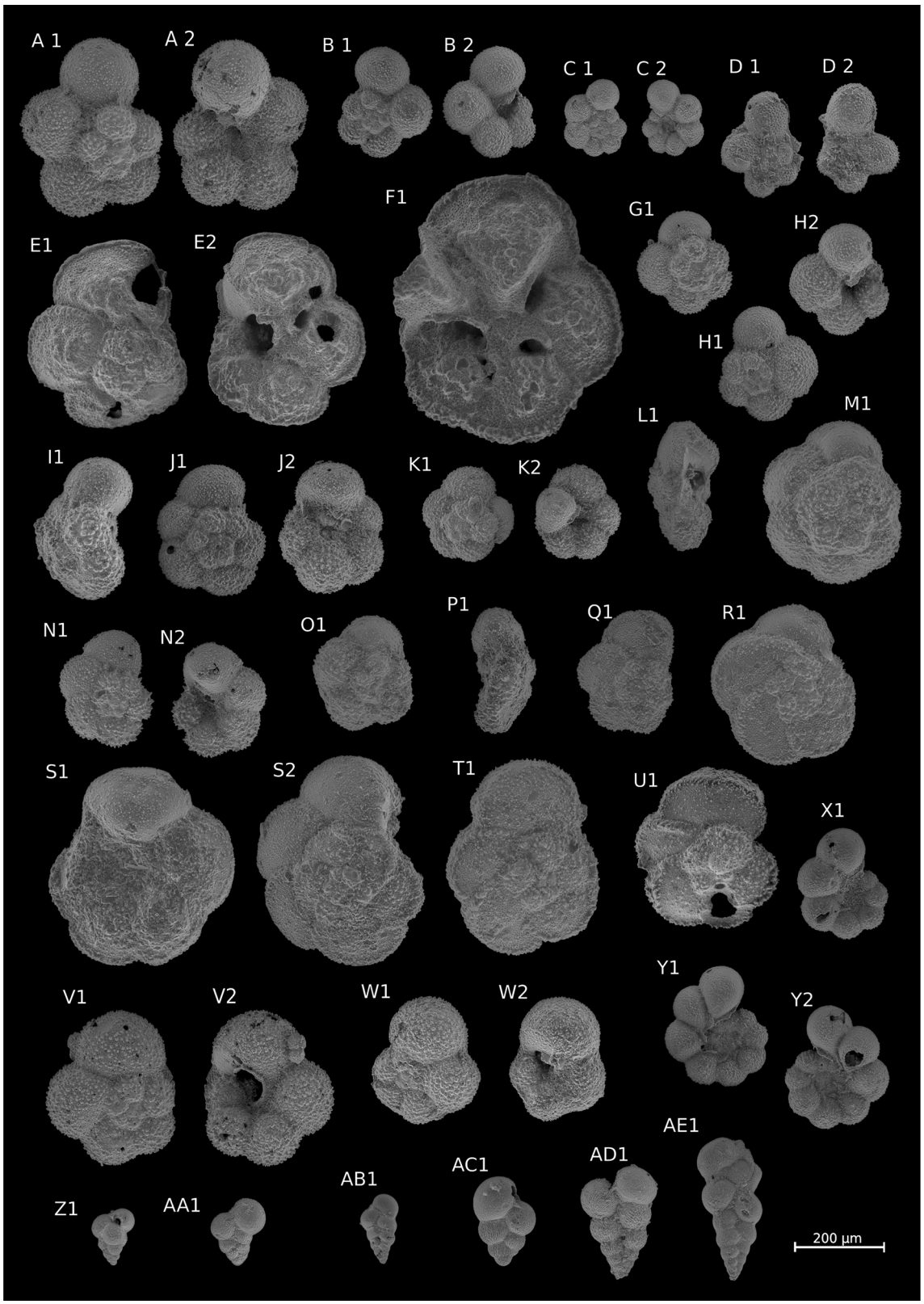
A 1
A 2
B 1
B 2
C 1
C 2
D 1
D 2
E1
E2
F1
G1
H2
H1
L1
M1
I1
J1
J2
K1
K2
N1
N2
O1
P1
Q1
R1
S1
S2
T1
U1
X1
V1
V2
W1
W2
Y1
Y2
AE1
AD1
AC1
AB1
AA1
Z1
200 µm

◀**Fig. 3** Planktonic foraminifera species in the Baltašiškė-267 (BA) and Bliūdsukiai-19 (Bl) boreholes: A1–A2 *Muricohedbergella delrioensis* (Carsey, 1926) dextral form (BA, 193.5 m depth); B1–B2 *M. delrioensis* (Carsey, 1926) sinistral form (BA, 193.5 m depth); C1–C2 *M. planispira* (Tappan, 1940) (BA, 197.0 m depth); D1–D2 *Clavihedbergella simplex* (Morrow, 1934) (Bl, 82.5 m depth); E1–E2 *Rotalipora cushmani* (Morrow, 1934) (BA, 193.5 m depth); F1 *Rotalipora cushmani* (Morrow, 1934) (BA, 193.5 m depth); G1 *W. inornata* (Bolli, 1957) (Bl, 78.0 m depth); H1–H2 *Whiteinella baltica* (Douglas and Rankin, 1969) (BA, 193.5 m depth); I1 *W. paradubia* (Sigal, 1952) (BA, 191.5 m depth); J1–J2. *W. archaeocretacea* (Pessagno, 1967) (BA, 192.5 m depth); K1-K2 *W. aumalensis* (Sigal, 1952) (BA, 192.5 m depth); L1 *Dicarinella algeriana* (Caron, 1966) (Bl, 83.2 m depth); M1 *Praeglobotruncana stephani* (Gandolfi, 1942) (Bl, 80.0 m depth); N1–N2 *P. delrioensis* (Plummer, 1931) (BA, 193.5 m depth); O1 *Dicarinella algeriana* (Caron, 1966) (Bl, 82.5 m depth); P1 *Dicarinella algeriana* (Caron, 1966) (Bl, 82.5 m depth); Q1 *Dicarinella algeriana* (Caron, 1966) (Bl, 83.2 m depth); R1 *D. canaliculata* (Reuss, 1854) (BA, 187.0 m depth); S1–S2 *D. imbricata* (Mornod, 1950) (Bl, 83.2 m depth); T1 *D. canaliculata* (Reuss, 1854) (Bl, 81.0 m depth); U1 *D. hagni* (Scheibnerova, 1962) (BA, 191.5 m depth); V1–V2. *Helvetoglobotruncana praehelvetica* (Reiss, 1957) (BA, 193.5 m depth); W1–W2 *Helvetoglobotruncana praehelvetica* (Reiss, 1957) (Bl, 82.5 m depth); X1 *Globigerinelloides ultramicrus* (Subbotina, 1949) (BA, 193.5 m depth); Y1–Y2 *G. bentonensis* (Morrow, 1934) (BA, 193.5 m depth); *Z1 Guembelitria cenomana* (Keller, 1935) *(BA, 198.5 m depth);* AA1 *Planoheterohelix paraglobulosa* (Georgescu and Huber, 2009) (BA, 198.5 m depth); AB1 *Planoheterohelix postmoremani* (Georgescu and Huber, 2009) (BA, 193.5 m depth); AC1 *Planoheterohelix paraglobulosa* (Georgescu and Huber, 2009) (BA, 193.5 m depth); AD1 *Planoheterohelix globulosa* (Ehrenberg, 1840) (BA, 198.5 m depth); AE1 *Planoheterohelix aff. moremani* (Cushman, 1938) (BA, 193.5 m depth)

benthic foraminifera. Fossils are absent in the intervals from 195.5 to 194.5 m and from 189.5 and 188.0 m in the Baltašiškė-267 core, and in the interval from 73.0 to 72.0 m in the Bliūdsukiai-19 core.

The upper Cenomanian to the lower Turonian or the Cenomanian–Turonian boundary (CTB) interval is traditionally divided into *Rotalipora cushmani* and *Whiteinella archaeocretacea* planktonic foraminiferal zones (Caron 1985; Robaszynski 1984; Robaszynski and Caron 1995) The C/T boundary is located in the *Whiteinella archaeocretacea* Zone according to the GSSP definition (Global Stratotype Section and Point) in Pueblo, Colorado and the nominate zone includes the interval with the OAE2 event (Luciani and Cobianchi 1999).

The stratigraphic distribution of the planktonic foraminiferal genera and species identified in Baltašiškė-267 and Bliūdsukiai-19 are shown in Fig. 2. The studied interval represents the Cenomanian–Turonian boundary interval. The planktonic foraminiferal assemblages occurring in the Baltašiškė-267 core were assigned to the upper Cenomanian *Rotalipora cushmani* Zone and to the uppermost Cenomanian-lowermost Turonian *Whiteinella archaeocretacea* Zone (from 193.5 to 187.0 m). The assemblages found in Bliūdsukiai-19 were assigned to the *Whiteinella archaeocretacea* Zone (from 83.2 to 72.0 m) following the planktonic foraminiferal zones proposed by Robaszynski and Caron (1995) for the Cretaceous in Europe and the Mediterranean.

The planktonic foraminiferal zones and the characteristics of their assemblages are presented below from the oldest to the youngest:

- *Rotalipora cushmani* Taxon Range Zone (TRZ). This zone spans from 198.5 to 193.5 m in the Baltašiškė-267 core. The upper part of the *Rotalipora cushmani* TRZ yield moderately diverse planktonic foraminifera (10 genera and 23 species) in the upper Cenomanian sediments. The index species *R. cushmani* is extremely rare in the studied interval. Rotaliporids were generally sparse in the studied region. In fact, the nominate species was not observed in previous studies (Aleksienė 2010). The low abundance of the deep dwelling *Rotalipora* species may have been due to ecological factors related to the prevalence of a relatively shallow environment (Keller and Pardo 2004) at the studied sites. Representatives of rotaliporids are just as rare in the upper Cenomanian sections in Bornholm, Poland and Bohemia (Kędzierski et al. 2012; Packer and Hart 1994; Peryt and Wyrwicka 1991; Ulicný et al. 1993; Vadja-Santivanez and Solakius 1999). Two well-preserved specimens of *R. cushmani* were found in the Baltašiškė-267 borehole (at a depth of 193.5 m). The upper limit of the *Rotalipora cushmani* TRZ can be defined by the first appearance (FA) of *Whiteinella archaeocretacea.* The FA of *W. aprica* at the same level (193.5 m) and the FA of *Dicarinella imbricata* one level higher (192.5 m) can be used as additional criteria.

The nominate zone is characterized by the presence of *Muricohedbergella* species (*M. delrioensis*, *M. portsdownensis*), *Whiteinella* species (*W. baltica*, *W. brittonensis*), *Praeglobotruncana* species (*P. delrioensis*, *P. sthephani*), *Globigerinelloides* spp. and heterohelicids (*Pl. globulosa*, *Pl. paraglobulosa*, and *Pl. postmoremani*). A single specimen of the double-keeled genus *Dicarinella* first appeared in this stratigraphic interval. The samples from the interval between 197.0 and 194.5 m are an exception; they contain very scarce planktonic and benthic foraminifera fauna, and 195.5 m sample is barren of foraminifera.

Moderately diverse benthic foraminifera (a total of 13 genera and 6 species) were identified in the upper Cenomanian-lower Turonian sediment succession. The benthic foraminiferal assemblage of the nominate *R. cushmani* Zone is characterized by high relative abundance of the calcareous genus *Bethelina*, the agglutinated genus *Arenobulimina*, and specially the species *Orthostella formosa.*

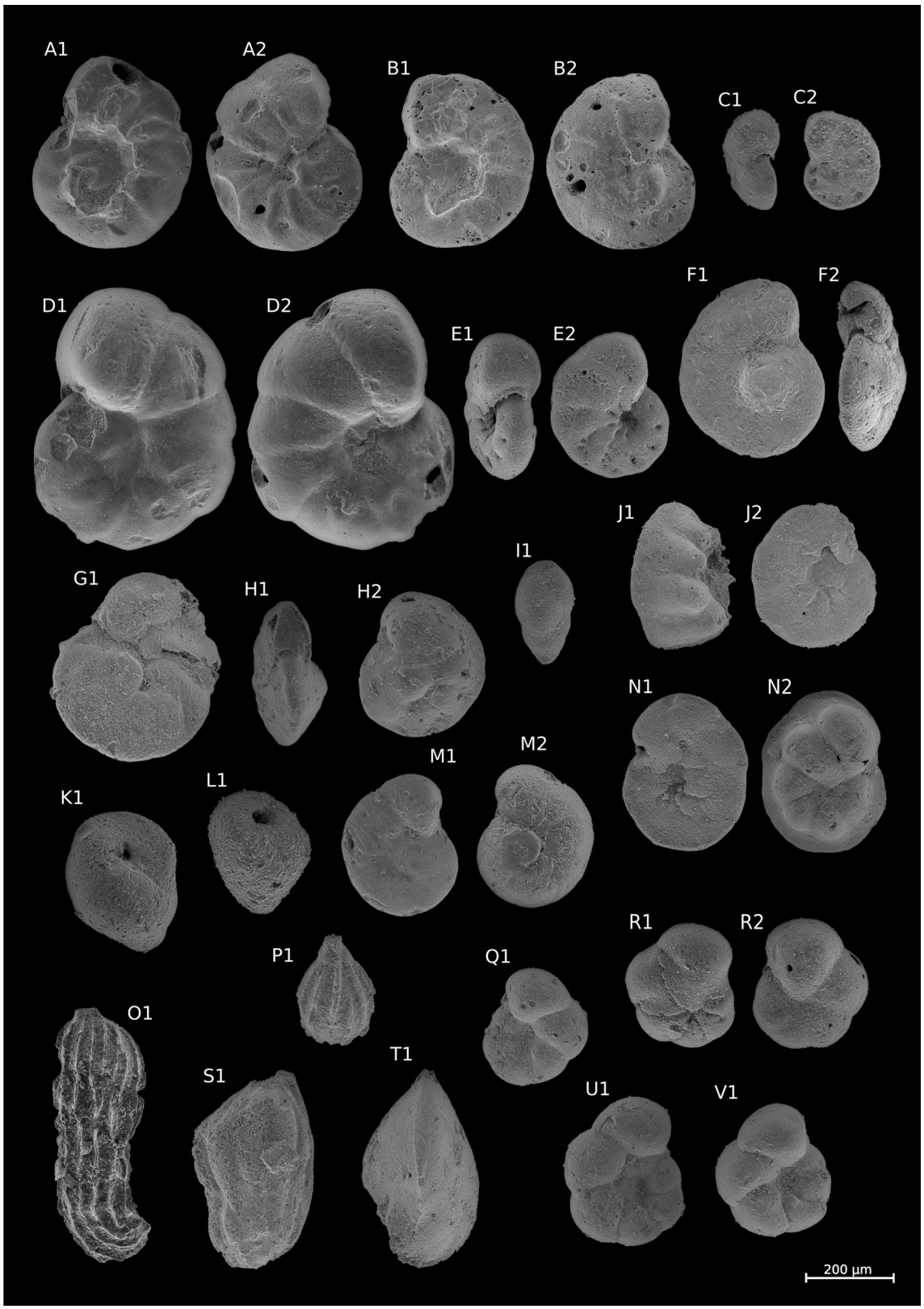
A1
A2
B1
B2
C1
C2
D1
D2
E1
E2
F1
F2
J1
J2
I1
G1
H1
H2
N1
N2
M1
M2
K1
L1
R1
R2
P1
Q1
O1
T1
S1
U1
V1
200 µm

◀**Fig. 4** Benthic foraminifera species in the Baltašiškė-267 (BA) and Bliūdsukiai-19 (Bl) boreholes: A1–A2 *Berthelina cenomanica* (Brotzen, 1942) (BA, 192.5 m depth); B1–B2 *B. cenomanica* (Brotzen, 1942) (BA, 192.5 m depth); C1–C2 *Berthelina* sp. *A.* (BA, 198.5 m depth); D1–D2 *B. baltica* (Brotzen, 1942) (BA, 192.5 m depth); E1–E2 *Berthelina* sp. *B.* (BA, 198.5 m depth); F1–F2 *Berthelina* sp. *C.* (Bl, 82.5 m depth); G1 *Berthelina* sp. *D.* (Bl, 82.5 m depth); H1–H2 *Berthelina* sp. *E.*(Bl, 79.0 m depth); I1 *Praebulimina elata* (Magniez-Jannin, 1975) (BA, 193.5 m depth); J1–J2 *Orithostella formosa* (Vasilenko, 1954) (BA, 198.5 m depth); K1 *Arenobulimina praesli* (Reuss, 1846) (BA, 198.5 m depth); L1 *Arenobulimina* sp. (BA, 198.5 m depth); M1–M2 *Berthelina* sp. *F.* (Bl, 78.0 m depth); N1–N2 *Orithostella formosa* (Brotzen, 1945) (BA, 198.5 m depth); O1 *Margulinopsis jonesi* (Reuss, 1862) (BA, 198.5 m depth); P1 *Lagena* sp. (BA, 193.5 m depth); Q1 *L. globosa* (Brotzen, 1954) (Bl, 82.5 m depth); R1–R2 *Lingulogavelinella orbiculata* (Kusnezova, 1953) (BA, 198.5 m depth); S1. *Margulinopsis* sp. (BA, 193.5 m depth); T1 *Saracenaria* sp. (BA, 193.5 m depth); U1 *L. globosa* (Brotzen, 1954) (Bl, 80.0 m depth); V1 *L. globosa* (Brotzen, 1954) (Bl, 75.0 m depth)

The dissapearence of *Bethelina cenomanica* (at 192.5 m) can be used as an additional criterion to set upper limit of the *R. cushmani* TRZ. *B. cenomanica* disappears either earlier or together with R. *cushmani* (Jarvis et al. 1988; Ulicný et al. 1993).

- The *Whiteinella archaeocretacea* Partial Range Zone (PRZ) spans from 192.5 to 187.0 m in Baltašiškė-267 and from 83.2 to 72.0 m in Bliūdsukiai-19. The zone may be characterized by the relatively high abundance of whiteinellids (*W. archaeocretacea*, *W. baltica*, *W. brittonensis*, *W. paradubia*, *W. aprica*, *W. aumalensis*, and *W. inornata*), the double-keeled genus *Dicarinella* (mainly *D. imbricata*), and the occurrence of *Helvetoglobotruncana praehelvetica*. In the middle part of the Bliūdsukiai-19 section (80.0–74.0 m) the foraminiferal assemblage is dominated by the genus *Whiteinella* (up to 60%). It is difficult to determine the upper boundary of the *Whiteinella archaeocretacea* PRZ, because studied samples are barren of *Helvetoglobotruncana helvetica.* As other authors mentioned (Hart et al. 2012) Tethyan taxon such as *Helvetoglobotruncana helvetica* probably is close to its northern limit as in Bornholm or UK and its appearance is influenced rather palaeocenographycally than stratigraphically.

The upper parts of both sections are characterized by the two benthic *Berthelina* and *Lingulogavelinella* genera. A characteristic feature of the foraminiferal assemblages in almost the entire Bliūdsukiai-19 section (the interval from 82.5 to 72.0 m) is an exceptional abundance of *L. globosa*.

5 $\delta^{13}C$ chemostratigraphy

The developed biostratigraphical framework enables the temporal tying of the $\delta^{13}C$ trend (Figs. 2, 6). The late Cenomanian part of the record (the *Rotalipora cushmani* Zone) was characterized by slightly positive values averaging 0.55‰. On the other hand, in the Cenomanian–Turonian boundary and the lower Turonian strata (the *W. archaeocretacea* Zone) carbonates are characterized by distinctly positive $\delta^{13}C$ values, averaging 2.64‰, with maximum values reaching 3.57‰. These very high values associated with typical foraminifera fauna of the C/T boundary, allow the interpretation that this $\delta^{13}C$ values correspond to the C–T stable isotopic excursion. Similar amplitudes above the $\delta^{13}C$ background values had been observed (Ogg et al. 2012; Kennedy et al. 2005).

6 Paleocommunity analysis

A community analysis of foraminifera by means of non-metric multidimensional scaling revealed some interesting trends in the compositional similarities between the samples and also in the ecological associations between separate species and genera (Fig. 5). It appears that the main axis revealing the most important gradient in compositions (NMDS1) generally reflects a temporal component of the compositional changes in species in both core sections. The samples from the Baltašiškė-267 core, which is represented by generally older samples from the *Rotalipora cushmani* Zone from the upper Cenomanian and *Whiteinella archaeocretacea* Zone from the Cenomanian–Turonian boundary, are mostly concentrated on the left side of the plot, where lower NMDS1 values prevail. On the other hand, most of the samples from the Bliūdsukiai-19 core are situated on the right side of the plot—on the opposite side of the major gradient. The later core is represented by younger strata from the *Whiteinella archaeocretacea* Zone and possibly still younger formations from the lower Turonian age in the uppermost part of the studied section. The variability on the second (NMDS2) axis is less clear, and probably reflects factors of secondary importance.

The revealed trend in the community compositions along NMDS1 could be explained by a long-term sea level rise during the Cenomanian, and especially the Turonian, which was detected based on the analyses of the facies distributions in southern Lithuania and north-eastern Poland (Grigelis and Leszczyński 1998). In the Lithuanian sections there are marked trends in the lithology during this transition, when the terrigenous material-rich marls of the Cenomanian age were replaced by the white chalks and

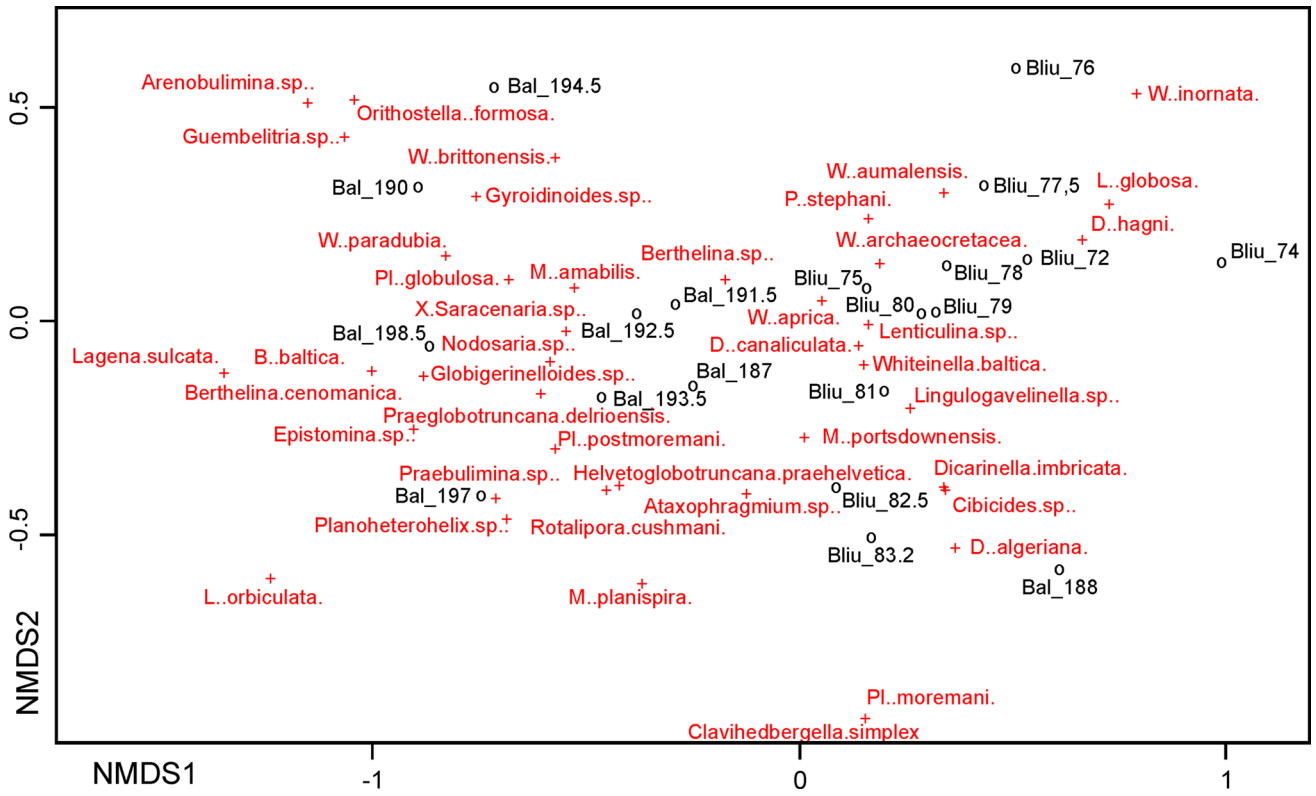

Fig. 5 Non-metric multidimensional scaling plot of the foraminifera samples (ovals), and species or genera (crosses) from the pooled analysis of the Bliūdsukiai-19 and Baltašiškė-267core data on the first two axes NMDS1 and NMDS2 [stress(unexplained variation) = 0.14]. The samples are indexed according to the names of the cores and the corresponding depth levels from which they were taken (e.g., Bal_187 reads as a sample from the Baltašiškė-267 core, taken from a depth of 187 m)

chalky marls of the Turonian age (Paškevičius 1997). This pattern implies sharp changes in the dominant sedimentological regime and in the physical and chemical properties of the water masses. As similar rising sea level trends have been revealed based on a compilation of sections from all over the world (Hallam and Wignall 1999; Haq 2014; Miller et al. 2003; Müller et al. 2008; Ogg et al. 2012), it is probable that this transgression was eustatic in origin. Therefore, biofacies tracking is an expected result of these global physical perturbations.

The changes in the species dominance patterns, as well as their evolutionary appearances and disappearances, could also be related to the globally recognized extinction episode at the Cenomanian–Turonian boundary and the related biogeochemical perturbation. Indeed, this proposition is confirmed by a comparison of the NMDS1 scores for sites with $\delta^{13}C$ values for whole rock carbonates (correlation analysis, gives $r = 0.75$ (with $N = 18$, and $p_{random} < 0.001$). Higher values of NMDS1 scores for sites are associated with higher $\delta^{13}C$ values.

The data on the coiling direction of *Muricohedbergella delrioensis* are sparse in this contribution, with only 18 samples, of which only 11 samples had 100 or more measurable specimens (Fig. 6). However, the present results are qualitatively similar to the patterns revealed by previous studies in lower latitudes (Desmares et al. 2016). At the end of the Cenomanian there was a sharp decrease in the number of sinistral forms in the Baltašiškė-267 section. Similarly, lower levels of sinistral forms were observed in the Bliūdsukiai-19 section, which spans the Cenomanian–Turonian boundary and therefore reflects a younger time interval (Fig. 6). In the upper Cenomanian *R. cushmani* Zone, the average sample percentage of sinistral shells is 36.47%, and in the uppermost Cenomanian-lowermost Turonian *W. archaeocretacea* Zone, this average percentage only reaches 22.39% (counts could be found in the Supporting information).

The results and observations presented here support the so-called "common cause hypothesis," which states that major changes in the biota and physical realm (sea level, climate, stable carbon isotopic excursions) are driven by common forcing mechanisms (Miller 1997; Peters 2005; Peters and Foote 2002). Therefore, despite the fact that marine ecosystems in higher latitudes were less affected by the C–T event (Gale et al. 2000; Keller et al. 2001), the effects on their faunal compositions, as evidenced by the multivariate and qualitative analyses presented here, are significant.

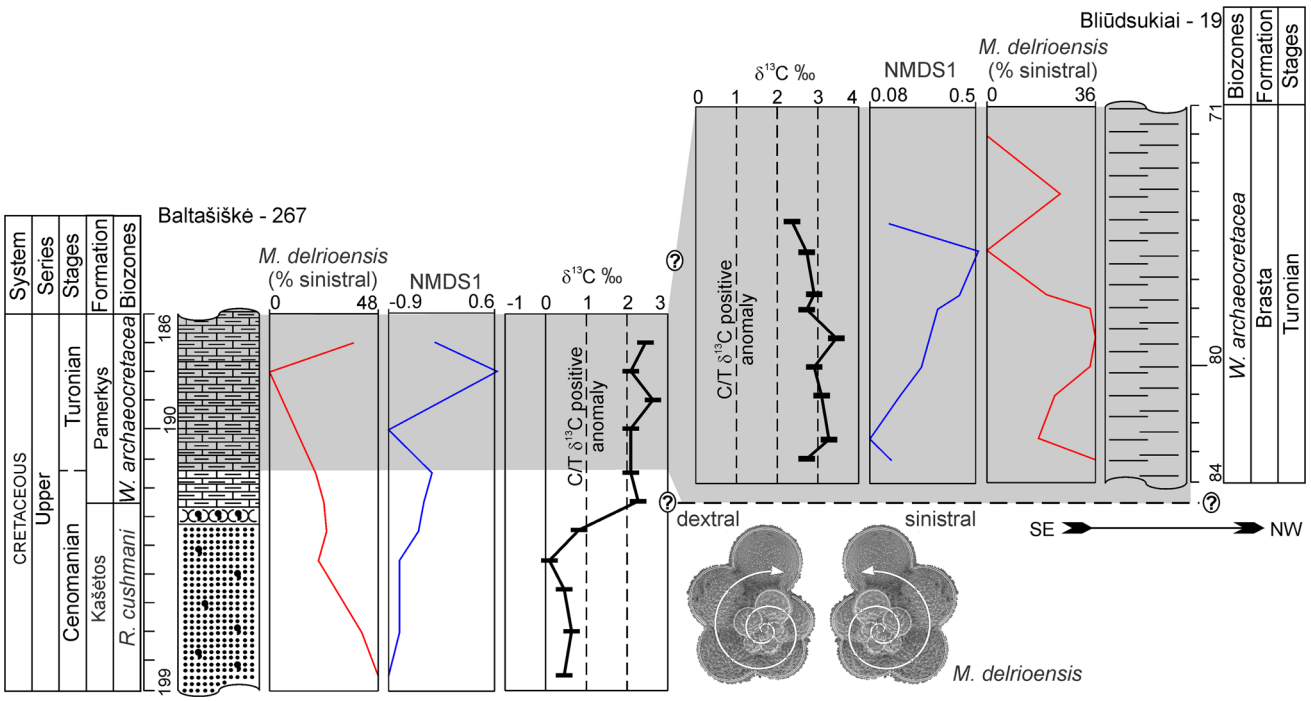

Fig. 6 Relationship between the $\delta^{13}C$ trend, proportion of the coiling directions in *Muricohedbergella delrioensis* (Carsey, 1926), and the NMDS1 axis scores in the Bliūdsukiai-19 and Baltašiškė-267 core samples

7 Conclusions

The integrated analysis of the Baltašiškė-267 and Bliūdsukiai-19 core sections revealed that the transition from the Cenomanian to the Turonian stages can be subdivided into two zones. The upper Cenomanian strata correspond to the *Rotalipora cushmani* Zone, and the C/T boundary and lowermost Turonian correspond to the *Whiteinella archaeocretacea* Zone. The positive stable carbon isotopic $\delta^{13}C$ excursion, with values > 2.00‰, is documented in the biostratigraphically expected position in the *Whiteinella archaeocretacea* Zone. Moreover, a comparison of the foraminiferal community states with the $\delta^{13}C$ trends revealed good correlation. This indicates the significant impact of the climate changes which prevailed during the transitions between the Cenomanian and Turonian epochs in the foraminiferal associations in northern temperate latitudes.

Acknowledgements We would like to thank two anonymous reviewers for their comments on the article and we also thank Gailė Žaludienė (Nature Research Centre, Vilnius) for her assistance with the SEM analyses of the samples.

References

Adnet, S., Cappetta, H., & Mertiniene, R. (2008). Re-evaluation of squaloid shark records from the Albian and Cenomanian of Lithuania. *Cretaceous Research, 29,* 711–722.

Aleksienė, A. (2010). Cenomanian–Coniacian upper cretaceous foraminiferal fauna of Lithuania. *Geologija, 52,* 9–15.

Bardet, N. (1994). Extinction events among Mesozoic marine reptiles. *Historical Biology, 7,* 313–324.

Bardet, N., Houssaye, A., Rage, J.-C., & Suberbiola, X. P. (2008). The Cenomanian–Turonian (late Cretaceous) radiation of marine squamates (Reptilia): the role of the Mediterranean Tethys. *Bulletin de la Société géologique de France, 179,* 605–622.

Batenburg, S. J., De Vleeschouwer, D., Sprovieri, M., Hilgen, F. J., Gale, A. S., Singer, B. S., et al. (2016). Orbital control on the timing of oceanic anoxia in the Late Cretaceous. *Climate of the Past, 12,* 1995.

Benson, R. B. J., Butler, R. J., Lindgren, J., Smith, A. S. (2010). Mesozoic marine tetrapod diversity: mass extinctions and temporal heterogeneity in geological megabiases affecting vertebrates. *Proceedings of the Royal Society of London B: Biological Sciences, 277*(1683), 829–834.

Caron, M. (1985). Cretaceous planktic foraminifera. In H. M. Bolli, J. B. Saunders, & K. Perch-Nielsen (Eds.), *Plankton stratigraphy* (pp. 17–86). Cambridge: Cambridge University Press.

Dalinkevičius, J. A. (1935). *On the fossil fishes of the Lithuanian Chalk: I.* Selachii: Vytauto Didžiojo Universitetas, Kaunas.

Desmares, D., Crognier, N., Bardin, J., Testé, M., Beaudoin, B., & Grosheny, D. (2016). A new proxy for Cretaceous paleoceanographic and paleoclimatic reconstructions: Coiling direction changes in the planktonic foraminifera Muricohedbergella delrioensis. *Palaeogeography, Palaeoclimatology, Palaeoecology, 445,* 8–17.

Eaton, J. G., & Kirkland, J. I. (2003). *Diversity patterns of nonmarine Cretaceous vertebrates of the western interior basin, high-resolution approaches in stratigraphic paleontology* (pp. 263–313). New York: Springer.

Eaton, J. G., Kirkland, J. I., Hutchison, J. H., Denton, R., O'Neill, R. C., & Parrish, J. M. (1997). Nonmarine extinction across the Cenomanian–Turonian boundary, southwestern Utah, with a

comparison to the Cretaceous–Tertiary extinction event. *Geological Society of America Bulletin, 109,* 560–567.
Elder, W. P. (1989). Molluscan extinction patterns across the Cenomanian–Turonian stage boundary in the Western Interior of the United States. *Paleobiology, 15,* 299–320.
Fraass, A. J., Kelly, D. C., & Peters, S. E. (2015). Macroevolutionary history of the planktic foraminifera. *Annual Review of Earth and Planetary Sciences, 43,* 139–166.
Gale, A. S., Jenkyns, H. C., Kennedy, W. J., & Corfield, R. M. (1993). Chemostratigraphy versus biostratigraphy: Data from around the Cenomanian–Turonian boundary. *Journal of the Geological Society, 150,* 29–32.
Gale, A. S., Smith, A. B., Monks, N. E. A., Young, J. A., Howard, A., Wray, D. S., et al. (2000). Marine biodiversity through the Late Cenomanian-Early Turonian: Palaeoceanographic controls and sequence stratigraphic biases. *Journal of the Geological Society, 157,* 745–757.
Grigelis, A. (1996). Lithostratigraphic subdivision of the Cretaceous and Palaeogene in Lithuania. *Geologija, 20,* 45–55.
Grigelis, A., & Leszczyński, K. (1998). Cretaceous: Stratigraphy and facies development: Geological and tectonic evolution. In S. Marek (Ed.), *Atlas of structural evolution of the Permian-Mesozoic complex of northeastern Poland, Lithuania and adjacent Baltic areas* (pp. 18–21). Warszawa: Polish Geological Institute.
Hallam, A., & Wignall, P. B. (1999). Mass extinctions and sea-level changes. *Earth-Science Reviews, 48,* 217–250.
Haq, B. U. (2014). Cretaceous eustasy revisited. *Global and Planetary Change, 113,* 44–58.
Harries, P. J. (2003). *A reappraisal of the relationship between sea level and species richness, high-resolution approaches in stratigraphic paleontology* (pp. 227–261). New York: Springer.
Harries, P. J., & Little, C. T. S. (1999). The early Toarcian (Early Jurassic) and the Cenomanian–Turonian (Late Cretaceous) mass extinctions: Similarities and contrasts. *Palaeogeography, Palaeoclimatology, Palaeoecology, 154,* 39–66.
Hart, M. B. (1999). The evolution and biodiversity of Cretaceous planktonic Foraminiferida. *Geobios, 32,* 247–255.
Hart, M. B., Bromley, R. G., & Packer, S. R. (2012). Anatomy of the stratigraphical boundary between the Arnager Greensand and Arnager Limestone (Upper Cretaceous) on Bornholm, Denmark. *Proceedings of the Geologists' Association, 123,* 471–478.
Hart, M. B., & Leary, P. N. (1991). Stepwise mass extinctions: The case for the Late Cenomanian event. *Terra Nova, 3,* 142–147.
Hasegawa, T., & Saito, T. (1993). Global synchroneity of a positive carbon isotope excursion at the Cenomanian/Turonian boundary: Validation by calcareous microfossil biostratigraphy of the Yezo Group, Hokkaido, Japan. *Island Arc, 2,* 181–191.
Jarvis, I., Carson, G. A., Cooper, M. K. E., Hart, M. B., Leary, P. N., Tocher, B. A., et al. (1988). Microfossil assemblages and the Cenomanian–Turonian (late Cretaceous) oceanic anoxic event. *Cretaceous Research, 9,* 3–103.
Jarvis, I., Lignum, J. S., Gröcke, D. R., Jenkyns, H. C., Pearce, M. A. (2011). Black shale deposition, atmospheric CO_2 drawdown, and cooling during the Cenomanian-Turonian Oceanic Anoxic Event. *Paleoceanography, 26*, PA3201. https://doi.org/10.1029/2010PA002081.
Jenkyns, H. C., Dickson, A. J., Ruhl, M., & Boorn, S. H. J. M. (2017). Basalt-seawater interaction, the Plenus Cold Event, enhanced weathering and geochemical change: Deconstructing Oceanic Anoxic Event 2 (Cenomanian–Turonian, Late Cretaceous). *Sedimentology, 64,* 16–43.
Kauffman, E. G., & Hart, M. B. (1996). *Cretaceous bio-events, Global events and event stratigraphy in the Phanerozoic* (pp. 285–312). New York: Springer.
Keller, G., Han, Q., Adatte, T., & Burns, S. J. (2001). Palaeoenvironment of the Cenomanian–Turonian transition at Eastbourne, England. *Cretaceous Research, 22,* 391–422.
Keller, G., & Pardo, A. (2004). Age and paleoenvironment of the Cenomanian–Turonian global stratotype section and point at Pueblo, Colorado. *Marine Micropaleontology, 51,* 95–128.
Kennedy, W. J., Walaszczyk, I., & Cobban, W. A. (2005). The global boundary stratotype section and point for the base of the Turonian stage of the Cretaceous: Pueblo, Colorado, USA. *Episodes-Newsmagazine of the International Union of Geological Sciences, 28,* 93–104.
Kerr, A. C. (1998). Oceanic plateau formation: a cause of mass extinction and black shale deposition around the Cenomanian–Turonian boundary? *Journal of the Geological Society, 155,* 619–626.
Kędzierski, M., Machaniec, E., Rodríguez-Tovar, F. J., & Uchman, A. (2012). Bio-events, foraminiferal and nannofossil biostratigraphy of the Cenomanian/Turonian boundary interval in the Subsilesian Nappe, Rybie section, Polish Carpathians. *Cretaceous Research, 35,* 181–198.
Li, Y.-X., Montañez, I. P., Liu, Z., & Ma, L. (2017). Astronomical constraints on global carbon-cycle perturbation during Oceanic Anoxic Event 2 (OAE2). *Earth and Planetary Science Letters, 462,* 35–46.
Luciani, V., & Cobianchi, M. (1999). The Bonarelli Level and other black shales in the Cenomanian–Turonian of the northeastern Dolomites (Italy): calcareous nannofossil and foraminiferal data. *Cretaceous Research, 20,* 135–167.
Meyers, S. R., Siewert, S. E., Singer, B. S., Sageman, B. B., Condon, D. J., Obradovich, J. D., et al. (2012). Intercalibration of radioisotopic and astrochronologic time scales for the Cenomanian–Turonian boundary interval, Western Interior Basin, USA. *Geology, 40,* 7–10.
Miller, A. I. (1997). Coordinated stasis or coincident relative stability? *Paleobiology, 23,* 155–164.
Miller, K. G., Sugarman, P. J., Browning, J. V., Kominz, M. A., Hernández, J. C., Olsson, R. K., et al. (2003). Late Cretaceous chronology of large, rapid sea-level changes: Glacioeustasy during the greenhouse world. *Geology, 31,* 585–588.
Müller, R. D., Sdrolias, M., Gaina, C., Steinberger, B., & Heine, C. (2008). Long-term sea-level fluctuations driven by ocean basin dynamics. *Science, 319,* 1357–1362.
Ogg, J. G., Hinnov, L. A., Huang, C. (2012). Cretaceous. In: F. M. Gradstein, J. G. Ogg, S. Mark, G. Ogg (Eds). The geologic time scale 2012 (pp. 793–853). Elsevier, Amsterdam.
Oksanen, J., Blanchet, F. G., Kindt, R., Legendre, P., Minchin, P. R., O'Hara, R. B., et al. (2015). Package 'vegan'. *Community ecology package, version, 2*(2-1), 1–280.
Orth, C. J., Attrep, M., Quintana, L. R., Elder, W. P., Kauffman, E. G., Diner, R., et al. (1993). Elemental abundance anomalies in the late Cenomanian extinction interval: A search for the source (s). *Earth and Planetary Science Letters, 117,* 189–204.
Packer, S. R., & Hart, M. B. (1994). Evidence for sea level change from the Cretaceous of Bornholm, Denmark. *GFF, 116,* 167–173.
Patzkowsky, M. E., & Holland, S. M. (2012). *Stratigraphic paleobiology: Understanding the distribution of fossil taxa in time and space*. Chicago: University of Chicago Press.
Paškevičius, J. (1997). *The geology of the Baltic Republics* (p. 387). Vilnius: Vilnius University and Geological Survey of Lithuania.
Peryt, D., & Wyrwicka, K. (1991). The Cenomanian–Turonian oceanic anoxic event in SE Poland. *Cretaceous Research, 12,* 65–80.
Peters, S. E. (2005). Geologic constraints on the macroevolutionary history of marine animals. *Proceedings of the National academy of Sciences of the United States of America, 102,* 12326–12331.

Peters, S. E., & Foote, M. (2002). Determinants of extinction in the fossil record. *Nature, 416,* 420–424.

Philip, J., Floquet, M., Platel, J. P., Bergerat, F., Sandulescu, M., Bara-Boshkin, E., Amon, E. O., Guiraud, R., Vaslet, D., Le Nindre, Y. (2000). Map 14—Late Cenomanian (94.7 to 93.5 Ma). Atlas Peri-Tethys, Palaeogeographical maps. CCGM/CGMW, Paris.

Prokoph, A., Villeneuve, M., Agterberg, F. P., & Rachold, V. (2001). Geochronology and calibration of global Milankovitch cyclicity at the Cenomanian–Turonian boundary. *Geology, 29,* 523–526.

R Development Core Team, 2015. R: A Language and Environment for Statistical Computing. Version 3.1.3. R Foundation for Statistical Computing, Vienna.

Robaszynski, F. (1984). Atlas of late Cretaceous globotruncanids. *Rev. Micropaleont., 26,* 145–305.

Robaszynski, F., & Caron, M. (1995). Foraminiferes planctoniques du Cretace; commentaire de la zonation Europe-Mediterranee. *Bulletin de la Société géologique de France, 166,* 681–692.

Ruban, D. A., Forster, A., Desmares, D. (2011). Late Cretaceous marine biodiversity dynamics in the Eastern Caucasus, northern Neo-Tethys Ocean: Regional imprints of global events. Geoloski anali Balkanskoga poluostrva, 29–46.

Sachs, S., Wilmsen, M., Knueppe, J., Hornung, J. J., & Kear, B. P. (2017). Cenomanian–Turonian marine amniote remains from the Saxonian Cretaceous Basin of Germany. *Geological Magazine, 154,* 237–246.

Sageman, B. B., Kauffman, E. G., Harries, P. J., & Elder, W. P. (1997). Cenomanian/Turonian bioevents and ecostratigraphy in the Western Interior Basin: contrasting scales of local, regional, and global events. In C. E. Brett & G. C. Baird (Eds.), *Paleontological events: Stratigraphic, ecological and evolutionary implications* (pp. 520–570). New York: Columbia University Press.

Sageman, B. B., Meyers, S. R., & Arthur, M. A. (2006). Orbital time scale and new C-isotope record for Cenomanian–Turonian boundary stratotype. *Geology, 34,* 125–128.

Sageman, B. B., Rich, J., Arthur, M. A., Dean, W. E., Savrda, C. E., Bralower, T. J. (1998). Multiple Milankovitch cycles in the Bridge Creek Limestone (Cenomanian–Turonian), Western Interior Basin.

Sakamoto, M., Venditti, C., Benton, M. J. (2017). 'Residual diversity estimates' do not correct for sampling bias in palaeodiversity data. *Methods in Ecology and Evolution, 8*(4), 453–459.

Schlanger, S. O., Arthur, M. A., Jenkyns, H. C., & Scholle, P. A. (1987). The Cenomanian–Turonian Oceanic Anoxic Event, I. Stratigraphy and distribution of organic carbon-rich beds and the marine δ13C excursion. *Geological Society, London, Special Publications, 26,* 371–399.

Schlanger, S. O., & Jenkyns, H. C. (1976). Cretaceous oceanic anoxic events: causes and consequences. *Geologie en Mijnbouw, 55,* 179–184.

Sepkoski, J. J. (1993). Ten years in the library: New data confirm paleontological patterns. *Paleobiology, 19,* 43–51.

Sinton, C. W., & Duncan, R. A. (1997). Potential links between ocean plateau volcanism and global ocean anoxia at the Cenomanian–Turonian boundary. *Economic Geology, 92,* 836–842.

Takahashi, A. (2005). Diversity changes in Cretaceous inoceramid bivalves of Japan. *Paleontological Research, 9,* 217–232.

Tsikos, H., Jenkyns, H. C., Walsworth-Bell, B., Petrizzo, M. R., Forster, A., Kolonic, S., et al. (2004). Carbon-isotope stratigraphy recorded by the Cenomanian–Turonian Oceanic Anoxic Event: Correlation and implications based on three key localities. *Journal of the Geological Society, 161,* 711–719.

Uličný, D., Hladiková, J., & Hradecká, L. (1993). Record of sea-level changes, oxygen depletion and the δ13C anomaly across the Cenomanian–Turonian boundary, Bohemian Cretaceous Basin. *Cretaceous Research, 14,* 211–234.

Vadja-Santivanez, V., & Solakius, N. (1999). Palynomorphs, foraminifera, and calcispheres from the greensand—limestone transition at Arnager, Bornholm: Evidence of transgression during the Late Cenomanian to Early Coniacian. *GFF, 121,* 281–286.

Yasuhara, M., Hunt, G., Cronin, T. M., Hokanishi, N., Kawahata, H., Tsujimoto, A., et al. (2012). Climatic forcing of Quaternary deep-sea benthic communities in the North Pacific Ocean. *Paleobiology, 38,* 162–179.